Korean J. Chem. Eng., 40(3), 488-496 (2023)
DOI: 10.1007/s11814-022-1321-y
pISSN: 0256-1115
eISSN: 1975-7220

INVITED REVIEW PAPER

Directing battery chemistry using side-view *operando* optical microscopy

S. Jayasubramaniyan and Hyun-Wook Lee†

School of Energy and Chemical Engineering, Ulsan National Institute of Science and Technology (UNIST),
50 UNIST-gil, Ulju-gun, Ulsan 44919, Korea
(*Received 11 September 2022 • Revised 4 October 2022 • Accepted 19 October 2022*)

Abstract−This review highlights recent progress and perspectives on side-view *operando* optical microscopy (OM) on lithium-ion batteries (LIBs). Side-view *operando* imaging studies on LIBs offer new insights for understanding the dynamic feature of battery chemistry since the images or movies offer direct visualization of the most realistic conditions. Taking advantage of a fundamentally complete understanding, we have a chance to overcome the formidable challenges of the LIBs. For the realistic demonstration of each part of the battery components, OM has been used to understand direct electrochemical reactions identifying the fundamental failure mechanisms that help overcome the challenges of LIBs. Here, we provide a comprehensive review of our research work in the field of the application of OM for understanding the various challenging aspects of LIBs. Moreover, we highlight that the further utilization of the OM technique towards and beyond the LIBs could lead to the development of next-generation batteries.

Keywords: *Operando* Optical Microscopy, Side-view Observation, *Operando* Observation, Electrode Observation, Lithium-ion Battery

INTRODUCTION

Energy storage is crucial because now it aims for a hyper-connected society where people, technology, and the environment interact [1-4]. In this regard, the concept of the 'Battery of Things (BoT) era' is coming, which means 'battery is everywhere,' like the Internet of Things (IoT), such as connected cars, online to offline, and biometric authentication [5-8]. Recently, interest in batteries for electric vehicles and wind or solar-based grid energy storage has been widely recognized as eco-friendly as well as hyper-connected systems for our daily life. To this end, energy density, power density, cycle life, and cost have been the major factors for high-energy and power batteries; therefore, LIBs have been intensively devoted to relieving such massive demands for widespread applications [9-12]. The emerging applications of wearable electronics, electric vehicles, and renewable energy integration require a quantum leap in battery performance that could offer high specific energy and long cycle life at low cost [13-16]. However, such significant challenges in developing new battery materials are the lack of understanding of electrode operation and its degradation. While various chemical species have been used to improve the cycling performance of traditional LIBs, their success in extending the cycle life of new battery chemistries has been relatively limited.

Operando analyses have provided several breakthroughs in the construction of high-performance materials and devices, including energy storage systems for the observation of nanoscale processes; chemical synthesis, electrochemical reaction, and physical interaction of various materials [17-20]. For the past decade, *operando* microscopy tools have contributed to understanding lithiation or sodiation behavior in battery materials for discovering new electrode materials with high performance and identifying the fundamental failure mechanisms that prevent a prolonged cycle life [21]. Although many previous studies of *in situ* X-ray and neutron diffractography, Raman, Fourier transform infrared spectroscopy, and nuclear magnetic resonance have illuminated the formidable and unknown questions of an electrochemical reaction, the spectroscopic methods have always been constrained from the ensemble-average information of the surface or bulk in the materials, which are not clear for the local degradation area [22,23]. In general, degradation phenomena occur in a local region that should be solved with a deeper understanding of its mechanisms and implications with tightening performance requirements in realistic configurations. Hence, direct imaging can offer exceptional opportunities for monitoring the dynamic processes of various electrode materials at a high spatial and temporal resolution to understand further the heterogeneity of the surface or bulk in electrochemically reacted samples [18].

Because there are many multiscale processes composed of mechanisms, we can categorize the major features and longings that manifest at different length scales and time variations, and proper imaging tools, as shown in Fig. 1. The broad category accounts for the coupling between the battery systems and constituting materials. For instance, as shown in Fig. 1(a), the length scales of the local composition of solid-electrolyte-interphase (SEI) at an anode could be a few nanometer scales, and the temporal scales could vary from less than a second to several hours. Observation of the heterogeneity of these SEI layers could provide a clue to finding the mechanism for stable intercalation reactions in graphite and plating/stripping reactions in metallic lithium anodes; nonetheless, this finding is one of the most challenging matters [24]. In the case of the related microscopy techniques (Fig. 1(b)), we must consider the limited image resolution by the wavelength of incident light or electron

†To whom correspondence should be addressed.
E-mail: hyunwooklee@unist.ac.kr

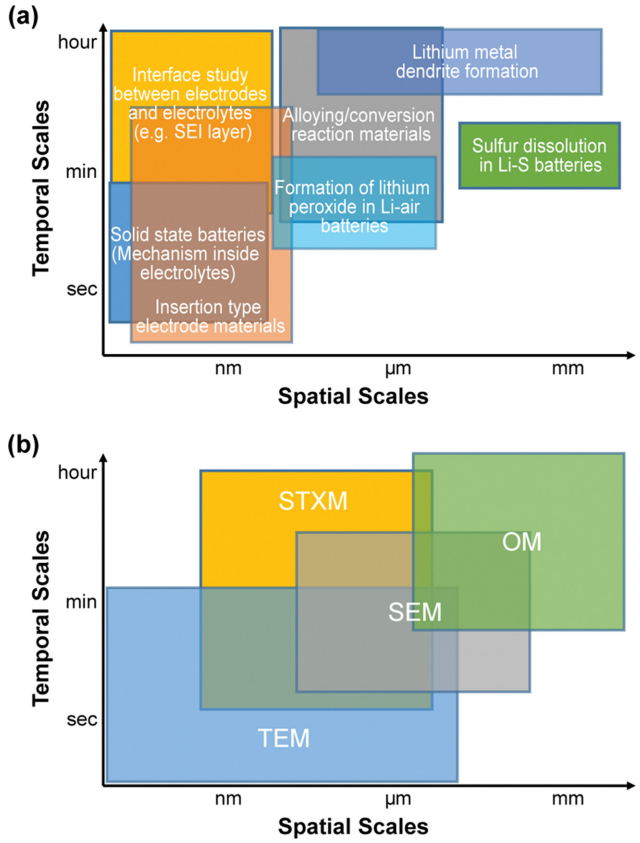

Fig. 1. Tentative temporal and spatial scales commensurate with (a) the representative issues in Li-ion, Li-S, Li-air, Li-metal, and ASS batteries, and (b) related microscopy techniques that can generally cover.

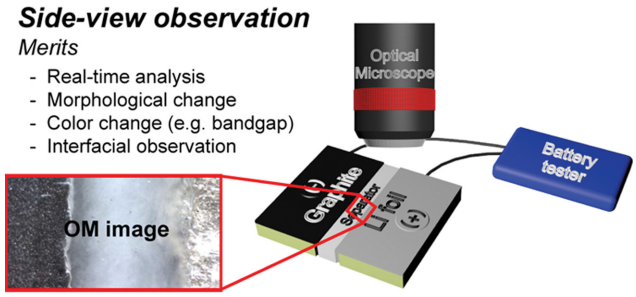

Fig. 2. Schematic illustration of a side-view *operando* OM cell. *Operando* OM allows the observation of the internal side-views of anodes, cathodes, electrolytes, and their interfaces. Reproduced from ref [44]. Copyright 2020 Wiley-VCH GmbH.

beam. Thus, the observable length scales of the wavelength of optical microscopy (OM) should be above a few hundred micrometers [25]. Employing electron and X-ray beams as light sources, such as transmission electron-, scanning electron- and scanning transmission X-ray-microscopy (TEM, SEM, and STXM), benefits from the spatial resolution up to nanometer scales. However, in addition to the temporal scales as an *operando* visualization, the intense incident beams are less favorable due to potential damages knocked by the short wavelength of electron or X-ray beams and the usability of the costly equipment [26].

To observe the various challenges of LIBs optically, different optical view set-ups, including planar view, side view, and cross-sectional view observation, were introduced over the years. The planar observation of the cell provides only the surface information of the electrode. However, despite the advances in electrode engineering, the formidable issues of lithium intercalation and deintercalation kinetics cannot be investigated by using planar observations [27]. The side-view OM set-up (Fig. 2) provides more realistic information about the electrode, including the dendrite growth and the kinetics of the Li-ion intercalation and deintercalation. So, depending on the experimental set-up, the structural change can be observed by the morphology and color of the sample, which indicates the optical bandgap change depending on the state of charge. In the case of *operando* optical microscopy, the most significant advantage is that we can employ the electrochemical cell as similar to the real cell configuration, which consists of liquid electrolytes and conventional electrodes. Therefore, this side-view configuration can be well used to analyze the effect of electrolytes and their additives [28].

Considering accessibility to compiling more realistic information on battery chemistry, this review mainly focuses on the studies on *operando* OM of LIBs and all-solid-state batteries (ASSBs). We have provided a comprehensive review of our research work in the field of the application of OM for understanding the various challenging aspects of LIBs. Moreover, we highlight that the further utilization of the OM technique towards and beyond the LIBs could lead to the development of high-energy and efficient batteries in the future.

IMPACT ON REPRESENTATIVE ANODES USING SIDE-VIEW *OPERANDO* OM

We focus on side-view operando OM studies for representative anode materials on LIBs, including those arising from physical deformation, color change, and volume expansion/shrinkage that reflect on the electrochemical reactions. The OM techniques are known to be limited in their space resolution that cannot be used to probe ion migration. Nevertheless, observing physical information, such as color, makes multi-technique approaches imperative for successful interpretation.

1. Lithium Metal Anodes

Li metal is considered a suitable anode material for developing high-energy batteries because of its high specific capacity (3,860 mAh/g) and low redox potential (–3.4 vs SHE). However, the high chemical reactivity of Li metal with liquid electrolyte leads to the formation of an undesirable SEI layer, which causes unsatisfactory battery cyclability and inferior rate capability [16]. Furthermore, Li dendrite formation and dead Li accumulation due to the inhomogeneous and uncontrolled Li deposition during the Li plating/stripping process leads to various safety concerns, including cell failure, poor Coulombic efficiency and thermal runway causing fire accidents, which impede the applicability of Li metal batteries in practical application [17].

Researchers have used various interface engineering strategies and electrolyte modification processes to stabilize the Li metal anode, including the formation of an artificial SEI layer, nanoscale interface layer coating, formation of Li alloy-based film, utilization of fluo-

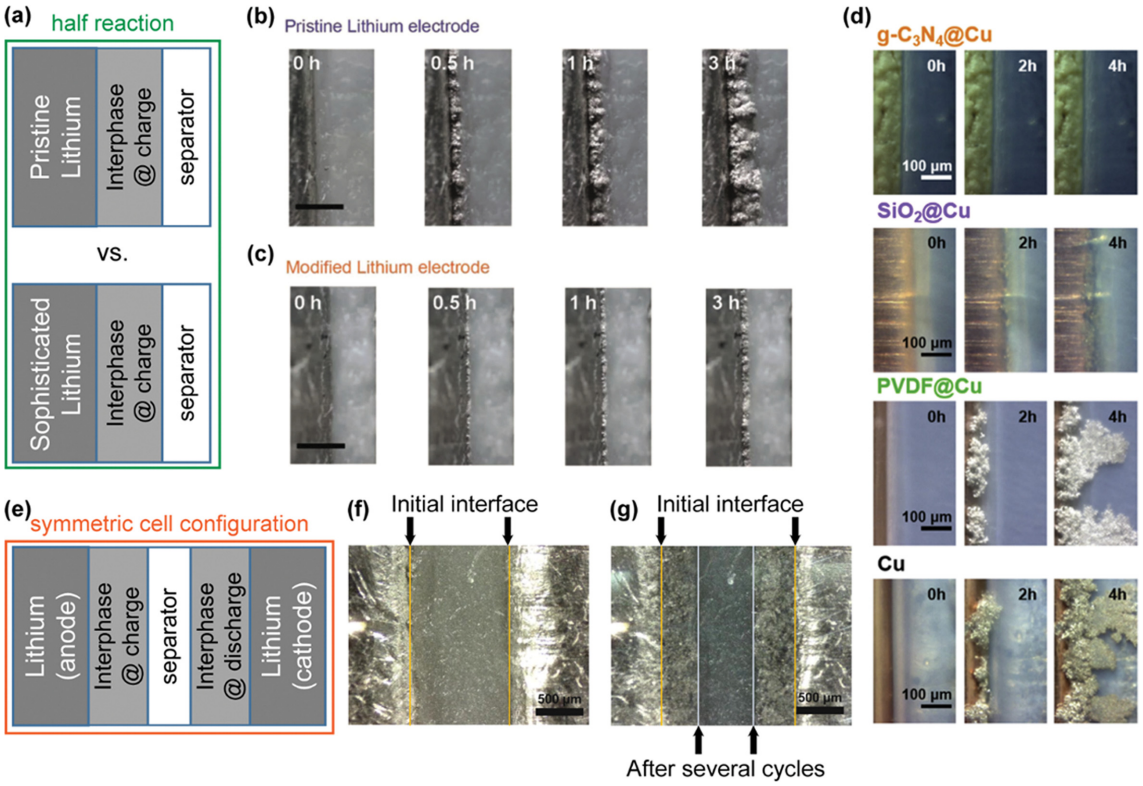

Fig. 3. (a) Schematic models illustrating the general observation of half-cell reactions at a side-view *operando* OM. During the lithium plating process, the interface between the separator and the electrode creates shows the formation of metallic lithium interphase, attributed to dendrites or uniform layers depending on sample conditions. Typical examples of (b) pristine and (c) modified lithium metal deposition visualized by side-view *operando* OM. Reproduced from ref [30]. Copyright 2018 Wiley-VCH GmbH. (d) Snapshots of four different electrodes during lithium metal plating on a pristine Cu current collector and modified Cu current collectors. Reproduced from ref [32]. Copyright 2020 Elsevier. (e) Scheme of the symmetric cell configuration. The symmetric configuration can compare the deposited thickness (f) before and (g) after several cycle tests.

rinated electrolyte and fluorine-containing additive and the effectiveness of the strategy has been investigated through various characterization methods [29]. Given the merits of the side-view *operando* OM technique, our research group utilized it for investigating the Li plating/stripping behavior, and dedicated considerable exertion to their development of lithium metal deposition [30-33]. The schematic models (Fig. 3(a)) illustrate the general observation of half-cell reactions at a side-view *operando* OM. The inhomogeneity on the lithium surface layer causes Li dendrite formation during the plating/stripping process. So, we investigated the effectiveness of the Li_xSi coating layer for dendrite suppression using OM. The OM results of the cell with Li_xSi coated Li metal showed uniform Li dissolution/deposition as compared to the bare Li metal (Fig. 3(b), (c)). The observed morphology of the Li deposition on the bare Li metal seems to be porous and Li dendrites were observed at 3 h. In contrast, a very dense and uniform Li deposition was observed for the Li_xSi coated Li metal and no dendrites were observed even after 3 h. The OM observation concludes that Li_xSi formation on the Li metal eliminates the inhomogeneity on the Lithium surface [30]. In general, lithiophic underneath growth has been considered a promising strategy to suppress the Li dendrite growth as compared with Lithiophic on-growth. So, we further utilized the *in situ* OM technique to validate the lithiophilic underneath growth strategy by observing the Li deposition behavior on the bare Cu, PVDF@Cu, SiO_2@Cu, and g-C_3N_4@Cu current collector (Fig. 3(d)). The OM results showed a completely different Li metal growth feature for the g-C_3N_4@Cu when compared with the bare and polymer-coated current collector. After 4h plating, the Li metal growth and dendrite growth were observed for all specimens except g-C_3N_4@Cu; thus, the restricted underneath growth due to the presence of lithiophilic g-C_3N_4 layer prevents the Li metal growth through it [32].

Taking advantage of the aforementioned observation of the direct metallic lithium deposition, the use of a symmetric cell configuration that is similar to a symmetric coin cell configuration can distinguish whether dendritic formation occurs and also quantify the deposited thickness of stable lithium metal deposition. The scheme in Fig. 3(e) shows a general symmetric cell configuration of metallic lithium electrodes. Using a symmetric configuration, deposition products during charge and discharge with a certain current density could be observed between the two interfaces. This allows quantifying the deposited thickness before and after several cycle tests, as shown in Fig. 3(f), (g). Considering an arithmetical calculation by a current density and deposited time, we could estimate the approximate thickness of the lithium deposition and compare the apparent density of the electrodes. In addition, this estimation could be a very versatile and promising platform for electrode or

electrolyte manipulation, especially for different electrolyte compositions, additives, media, etc.

2. Silicon-based Anodes

Although silicon (Si) anodes have received great attention for LIBs due to the high gravimetric energy density, high-percent utilization of Si anodes is still challenging considering the practical volumetric energy density (Wh/liter) [34]. So, small amounts of Si less than 10% are considered a plausible solution combined with graphite anodes. The Si content has a certain ratio to alleviate capacity fading up on cycling caused by the volume expansion, leading to particle cracks and disconnection [35]. From a practical perspective, the volume expansion of the particles generates the total volume expansion of Si anodes [36]. However, mostly, during the delithiation process, the Si electrode would not recover the original volume space, resulting in less interaction with each other. The reduced interaction causes to increase the electrical resistance of the electrode, leading to joule heating of the electrode, attributed to possible danger, such as an explosion [37]. The visualization of physical volume expansion of Si electrodes is relatively easy, even though particle expansion is at least submicron scales, as shown in Fig. 1(a). So, our group used the OM technique to visualize the volume expansion of micron-sized Si electrodes and densified Si/C composite electrodes (Fig. 4(a)-(d)). The OM observations of the Si anode showed rapid volume expansion during lithiation, but the original volume of the electrode was not recovered during the delithiation process. In contrast, the densified Si/C composite electrode showed relatively less volume expansion than the bare Si electrode and the original volume of the electrode was retained after the delithiation process. Overall, the OM observation demonstrates that the densified Si/C composite electrode successfully accommodates the volume expansion during the lithiation and del-lithiation process [38].

To overcome the volume expansion-induced issues in silicon anodes, one effective approach could be the utilization of an effective binder to improve the interconnection between the particles and provide better particle adhesion than the conventional binder of carboxymethyl cellulose (CMC) with the aid of styrene butadiene rubber (SBR) after repeated cycling and high integrity of Si [39,40]. So, our group prepared a novel water-soluble binder using three functional materials; thus we denoted this novel binder "DPA binder", as it utilizes DMA-PEG-Acrylate functional units. (i) poly(ethylene glycol)-diacrylate (PEGDA) unit provides good structural integrity and high machinal strength, which could alleviate the external stresses induced by the volume expansion of Si particles, (ii) dopamine methacrylate (DMA) unit improves the addition between Si particle, conductive agent and current collector with the help of its catechol functional groups, (iii) poly (ethylene glycol) monomethyl ether-acrylate (PEG) promotes the Li^+ transport (Fig. 4(e)). Further, we used the OM technique to validate the advantages of the novel binder for the volume expansion issues related to the Si anodes. The obtained OM result of the commercial SBR-CMC binder and novel DPA binder during lithiation and de-lithiation (Fig. 4(f)) shows that our novel binder with its synergetic functionality of three units effectively suppresses the volume expansion and reduces the microstructural changes of the Si electrode as compared with Si electrode with commercial SBR-CMC binder [41].

3. Graphite Anodes

The commercial Li-ion technology still uses graphite as the most predominant anode material because of its high safety as compared

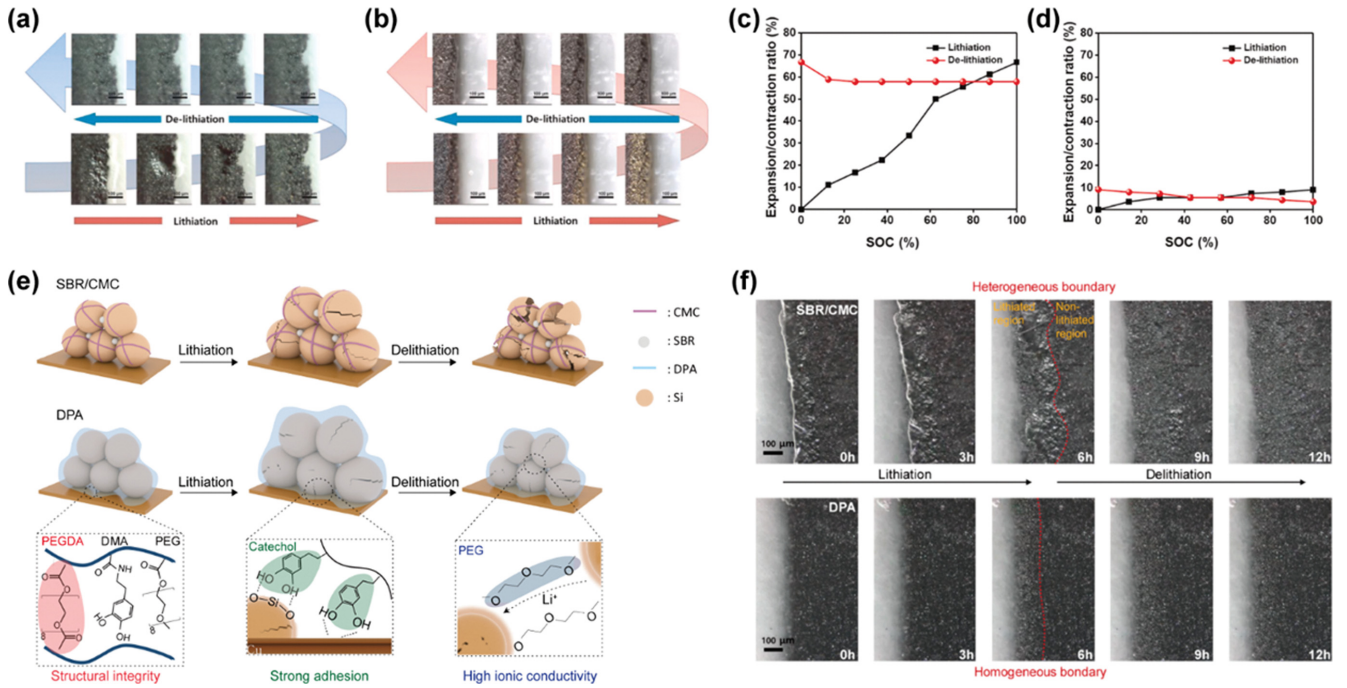

Fig. 4. Side-view *operando* OM observations of (a) silicon and (b) silicon/graphite composite. Expansion and contraction ratio of both electrodes (c), (d), respectively. Reproduced from ref [38]. Copyright 2021 Elsevier. (e) Schematic of different binders that influence particle integrity, resulting in the electrode expansion and contraction ratio, and (f) their snapshots of silicon electrodes with SBR/CMC (top) and DPA (bottom) binders.Reproduced from ref [41]. Copyright 2022 American Chemical Society.

with Li metal anode. However, understanding its kinetics during the charge-discharge process at the electrode level is still challenging; this leads to the researcher's interest in the direct observation of graphite anodes [42-45]. Considering the merits of the side-view *operando* OM technique, our group has utilized the OM analysis to directly observe the kinetics of graphite anode during the lithiation and de-lithiation process. First, we analyzed the optical property of the lithiated graphite by measuring the optical reflectivity using UV/Vis spectroscopy and the correlation between energy gap variation with the SOC and DOD determined by the Ku-Belka-Munk theory [43]. The results of band gap structure analysis at the π band of graphite before and after lithiation showed that the fermi level of lithiated graphite (LiC_6) is comparatively higher than the initial stage of lithiation (Fig. 5(a)), because when lithiation occurs the electron prefers to stay within the graphite π band, which means that Fermi level lies within the graphite π band at the initial stage. When lithiation occurs, the band gap between the two slaps of the graphite increases from 3.35 to 3.7A^{o} (Fig. 5(b)), because the intercalation of Li ion into the slap induces the overlapping of the adjunct π orbitals, thus causing the weak bonding. The color changes of the graphite electrode during lithiation are mainly caused by the changes in the energy gap due to the Li-ion intercalation (Fig. 5(c)).

Furthermore, the side view OM analysis exhibited color variation at the separator/electrode interface during the lithiation and de-lithiation process (Fig. 5(d)). When lithiation occurred, the graphite electrode color changed initially to red at the interface and then to yellow under the fully lithiated state, and the reversible color changes were observed during the delithiation process. Moreover, the hysteric behavior observed in the plot against the lithiated graphite distance and time revealed the more Li diffusion occurs during the charge state (Fig. 5(e)). In addition to OM, we have collected Raman spectra of the graphite anode for the fully lithiated state (point 1), partially lithiated state (Point 2, 3) and unlithiated state at the different sites during lithiation (Fig. 5(f), (g)). The results indicate that the intensity of the D band, which describes the breathing mode of the Sp2 carbon atom in the ring, increases from point 4 to 1, which implies that the lithiation process leads to more defects in the graphite structure. Overall, the side-view OM analysis sufficiently revealed the charge-discharge kinetics of the graphite anode [44].

OPPORTUNITIES VISUALIZED BY *OPERANDO* OM FOR BEYOND LITHIUM-ION BATTERIES

In this section, we summarize the application of OM for addressing the various challenging issues associated with the energy storage systems beyond the LIBs, such as all solid-state batteries (SSBs) and Li-sulfur (Li-S) batteries.

1. All-solid-state Batteries

A promising approach to minimize the safety issues related to the current Li-ion battery is replacing the highly flammable liquid electrolyte with a non-flammable solid electrolyte. The utilization of SE also allows the stacking of the multiple cells together, thus increasing the energy density of the battery pack, which is needed for the high range electric vehicles (EVs). Hence, the beneficial advantages of the solid-state battery (SSBs) have generated increasing

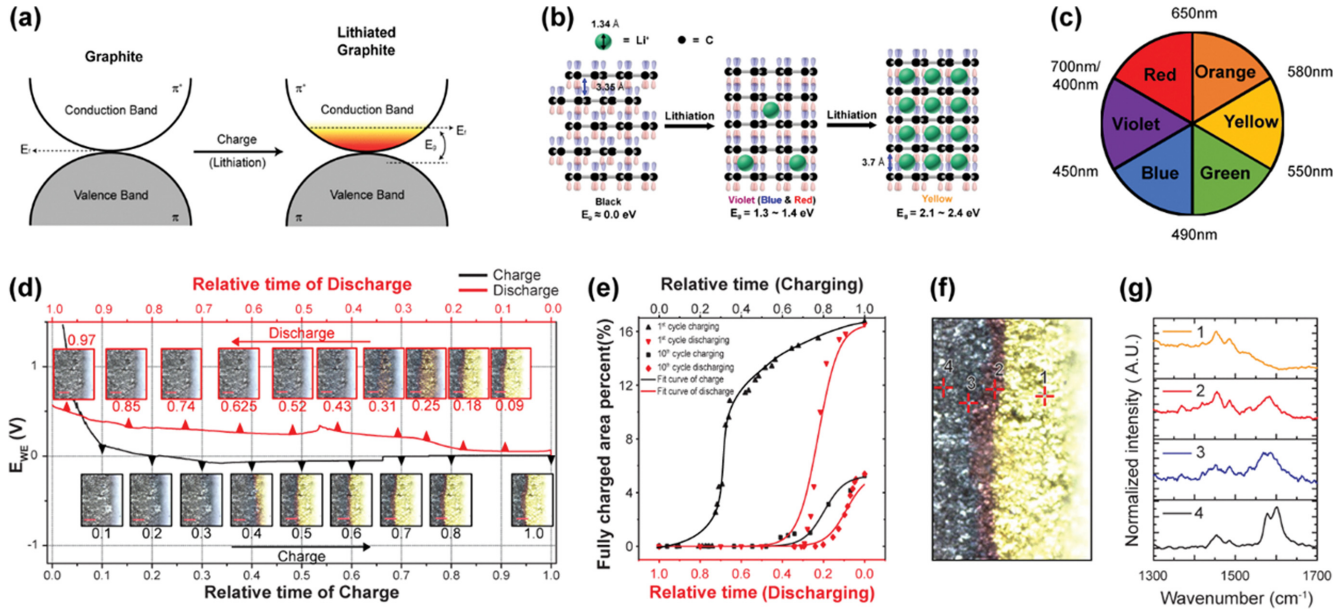

Fig. 5. (a) Schematic that pinpoints the origin showing color of band gap structure at π band of graphite before (left) and after (right) lithiation. (b) Schematic of the internal structure of the graphite anode during lithiation. (c) Color wheel with the wavelength ranges of each color; opposite colors in the wheel are complementary colors. When some wavelength of incident light is absorbed, the color complementary to the absorbed color appears. (d) Side-view *operando* OM images (insets; scale bars represent 100 mm) of a graphite electrode during lithiation and its voltage profilefor the 1st charge-discharge cycle. (e) Relative depth of charge as a function of the relative charge and discharge times for the 1st and 10th charge-discharge cycles. (f) Side-view *operando* OM image during an electrochemical reaction and (g) its Raman spectra of the points marked in (f): point 1 corresponds to the fully lithiated state, points 2 and 3 are partially lithiated states, and point 4 represents the unlithiated state. Reproduced from ref [44]. Copyright 2020 Wiley-VCH GmbH.

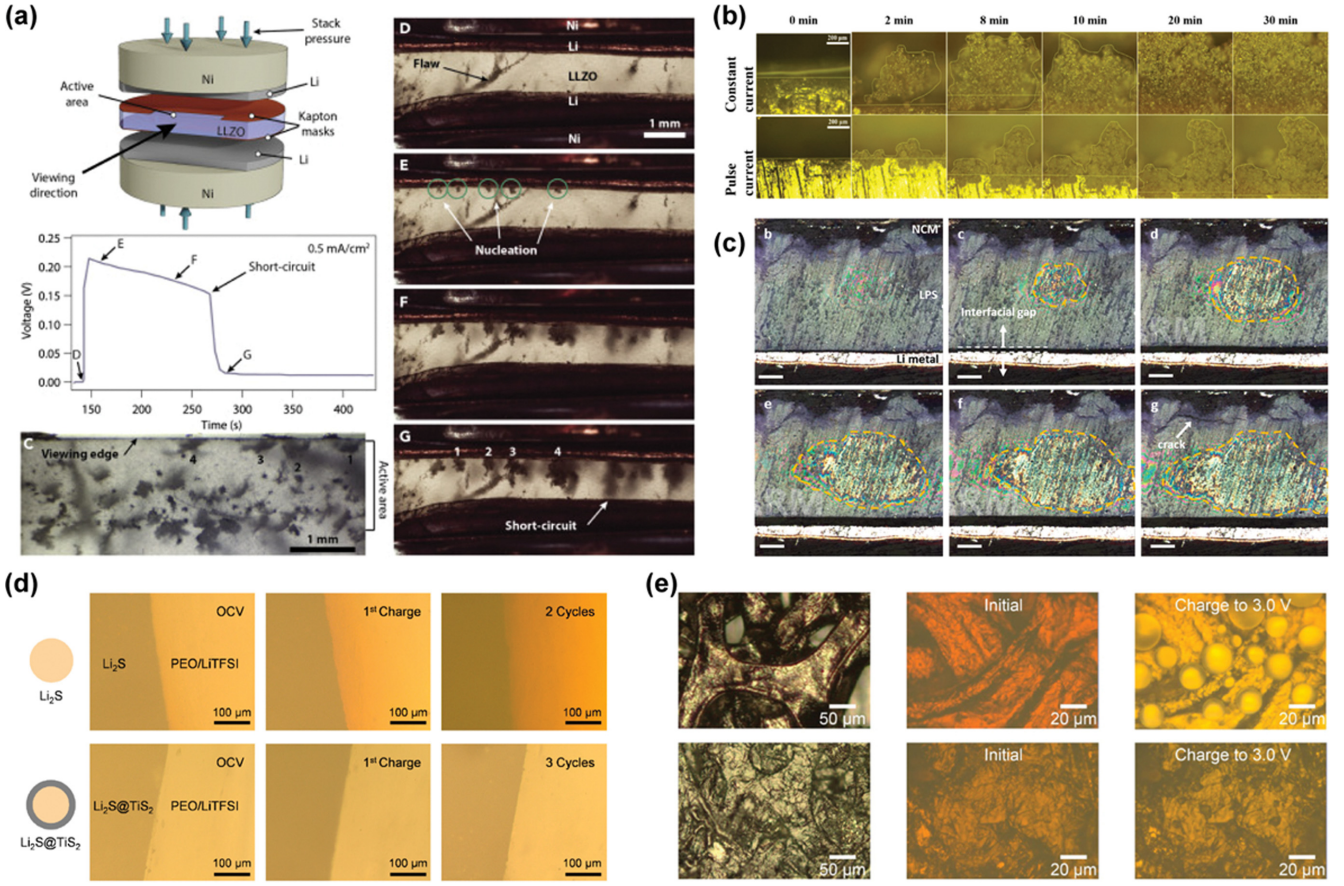

Fig. 6. (a) Schematic of cell geomertry for OM observation, voltage profile and OM images of the cell at the different points of voltage profile Reproduced from ref [52]. Copyright 2020 Elsevier Inc. (b) OM images of the Li metal/SE interface observed under the constant current and pulse current charging mode. Reproduced from ref [53]. Copyright 2020 American Chemical Society. (c) OM images of the observation of Li deposition in the SE, densdrite fromation and growth at the Li metal/SE interface. Reproduced from ref [54]. Copyright 2021 American Chemical Society. (d) OM images of the Li_2S/SE and $Li_2S@TiS_2$/SE interface during the cycling process. Reproduced from ref [56]. Copyright 2020 American Chemical Society. (e) OM images of the observation sulfur droplet on Ni foam and sufulr crystals on the carbon coated Ni foam. Reproduced from ref [57]. Copyright 2020. American Association for the Advancement of Science's (AAAS).

research attention in the designing and development of all SSBs with high efficiency [46-48]. Although the SSBs are the best candidates for future electric vehicle application, the interfacial instability of SE with electrode material and Li filament formation inside the SE leads to cell failure, which hinders the applicability of SSBs in EV, and researchers have used various advanced *in situ* characterization techniques to visualize the Li filament formation and to address the interface issues [49,50].

However, the investigation of the interfacial changes and the effect of Li filament formation during the battery operation is very important because batteries are dynamic devices, and the electrode and SE are not in equilibrium during the operation [51]. From this point of view, operando side-view OM has received much attention because it can provide plenty of information about the changes occurring inside the electrode and at the SE/electrode interface during operation. Dasgupta et al. [52] observed the Li filament formation inside the Garnet-based LLZO SE using operando OM microscopy (Fig. 6(a)). The results indicate that Li filament formation was observed at high current density and the propagation of Li filaments leads to the machinal crack formation and further growth leads to a short circuit. A similar research group investigated the Li transportation bath in the solid-state composite electrolyte by observing the color changes of the composite electrode using the operando OM technique. The OM observation results concluded that Li transportation in the composite electrode occurs through two different pathways: Li transport via SE and Li diffusion within the graphite electrode [53].

Sun et al. [53] observed Li-dendrite formation in SSBs under two different charging modes (constant current and pulsed current) using *in situ* OM analysis. The OM images clearly showed that the Li dendrite formation and propagation were very fast at the constant current mode than in pulsed current mode, and it was found that the pulsed current charging method could suppress the Li dendrite formation (Fig. 6(b)). Recently, Lu et al. [54] visualized the Li growth behavior inside the SE and observed the Li deposition inside the SE using the *in situ* OM technique. Furthermore, the OM results (Fig. 6(c)) revealed that the Li deposition and dendrite propagation inside the SE are the main causes of the crack forma-

tion and cell failure of SSBs.

2. Lithium-sulfur Batteries

The high demand for batteries with sufficient energy density for the next-generation electric vehicle has triggered battery research toward the development of high-energy battery systems beyond the current Li-ion battery technology [10]. In this regard, Lithium-sulfur batteries (Li-S) have been considered a suitable candidate to meet the energy density requirements of electric vehicles due to their high energy density (2,500 $Whkg^{-1}$) and the low cost of sulfur. However, the practical utilization of Li-S batteries in EVs is hindered by various factors, including the low electronic conductivity of sulfur and Li_2S increases the activation energy of the redox process. In addition, the shuttle effect of polysulfides during the redox process leads to rapid capacity loss and low Coulombic efficiency. Various strategies have been applied to overcome the challenging issues of Li-S battery, including the utilization of carbonaceous material as the host material to improve electric conductivity as well as trapping the sulfur and polysulfides species, and various separator modifications were applied to suppress and block the polysulfide diffusion [55].

Various *in situ*/*operando* characterization techniques have been utilized to investigate the solid phase formation and dissolution of sulfur and Li_2S, morphological changes and tracking the polysulfide diffusion during the charge-discharge process [56,57]. Recently, the OM technique has been used to investigate the challenging issues related to the Li-S battery. Cui et al. used OM to investigate the applicability of the nanoscale encapsulation strategy which has been widely used in liquid electrolyte systems to solid state Li-S batteries. The OM observation (Fig. 6(d)) implies that the TiS_2 encapsulation of Li_2S particle sufficiently suppresses the polysulfide dissolution [56]. Furthermore, the same group used the OM technique to visualize sulfur growth in real-time on the various current collector during battery operation. The OM observation (Fig. 6(e)) showed the formation of supercooled sulfur droplets on the nickel current collector and the strong interaction between Ni and lithium polysulfides reduces the polysulfide shuttle effect and improves the Li_2S phase conversion kinetics [57].

SUMMARY AND OUTLOOK

This review has summarized our research work towards the utilization of side-view OM for the investigation of challenging issues of the LIBs and various research works which have used the OM for the investigation beyond LIBs such as all-solid-state batteries and Li-sulfur batteries. The above discussion of the available research reports concludes that OM analysis is a promising technique for the investigation of the charge-discharge kinetics and SEI degradation mechanism of the LIBs. Further, the OM analysis provides sufficient scientific information about dendrite propagation and instability of the SEI layer formed on the Li metal anode in Li-metal batteries. In addition to LIBs, the OM analysis was widely used for the investigation of interface degradation mechanism, dendrite evolution and mechanical failures of all-solid-state batteries. Recently, OM technologies have been applied to Li-sulfur batteries for the dynamic investigation of polysulfide conversion and diffusion kinetics. Also, the OM tools have been widely used for investigating and understanding lithiation or sodiation behavior in battery materials for discovering new electrode materials with high performance and identifying the fundamental failure mechanisms. Overall, the OM analysis is a suitable technique for addressing the various issues of energy storage devices.

In general, lithiation and de-lithiation behavior has been explained by the diffusion kinetics by the fundamental viewpoints at a single-particle level. However, we have to consider that the degree of lithiation occurs from the top surface to the bottom electrode across pseudo-2-dimensional models with porous structures. Once most commercial electrodes aim to approach high mass loading and tap density, the complex mechanism behind this remains subject to debate. Hence, the macro-scale observation, such as side-view *operando* OM techniques, could give information on the charged degree of the entire particles of the whole electrode by analyzing the physical deformation of the top surface. Also, the merits of such imaging observations are very direct against the ensemble averages. Most degradation happens from a local region of an electrode, which in turn requires greater experimental precision to ascribe physical meaning to the degradation parameters. Apart from the difficulties described above, we believe that the further utilization of the OM technique towards and beyond the LIBs will provide more insightful information and scientific solution for the challenging issues associated with batteries, which could lead to the development of high-energy and efficient batteries for the next-generation energy devices.

ACKNOWLEDGEMENTS

This work was supported by the 2022 Research Fund (1.220022.01) of UNIST and Individual Basic Science & Engineering Research Program (2019R1C1C1009324) through the National Research Foundation (NRF) of Korea funded by the Ministry of Science and ICT (MSIT).

CONFLICT OF INTEREST

The authors declare no competing financial interest.

REFERENCES

1. P. Simon and Y. Gogotsi, *Nat. Mater.*, **19**, 1151 (2020).
2. D. Son, J. Kang, O. Vardoulis, Y. Kim, N. Matsuhisa, J. Y. Oh, J. W. To, J. Mun, T. Katsumata, Y. Liu, A. F. McGuire, M. Krason, F. Molina-Lopez, J. Ham, U. Kraft, Y. Lee, Y. Yun, J. B.-H. Tok and Z. Bao, *Nat. Nanotechnol.*, **13**, 1057 (2018).
3. S. Niu, X. Wang, F. Yi, Y. S. Zhou and Z. L. Wang, *Nat. Commun.*, **6**, 8975 (2015).
4. R. Saroha, J.-H. Ahn and J. S. Cho, *Korean J. Chem. Eng.*, **38**, 461 (2021).
5. K.-H. Choi, J. T. Yoo, C. K. Lee and S.-Y. Lee, *Energy Environ. Sci.*, **9**, 2812 (2016).
6. J. Shi, S. Liu, L. Zhang, B. Yang, L. Shu, Y. Yang, M. Ren, Y. Wang, J. Chen, W. Chen, Y. Chai and X. Tao, *Adv. Mater.*, **32**, 1901958 (2020).
7. M. K. Jeon, S.-W. Kim, H.-C. Eun, K. Lee, H. Kim and M. Oh,

Korean J. Chem. Eng., **39**, 1472 (2022).
8. H. H. Oh and J. Joo, *Korean J. Chem. Eng.*, **38**, 1052 (2021).
9. Y. Yu, G. Li, S. Zhou, X. Chen, H.-W. Lee and W. Yang, *Carbon*, **120**, 397 (2017).
10. J. H. Yun, J. H. Kim, D. K. Kim and H.-W. Lee, *Nano Lett.*, **18**, 475 (2018).
11. S. A. Ahad, R. Pitchai, A. M. Beyene, S. H. Joo, D. K. Kim and H.-W. Lee, *ChemSusChem.*, **11**, 3402 (2018).
12. B. Moorthy, J. H. Kim, H.-W. Lee and D. K. Kim, *Energy Storage Mater.*, **24**, 602 (2020).
13. J. Ryu, D. Hong, H.-W. Lee and S. Park, *Nano Res.*, **10**, 3970 (2017).
14. Y. Sun, L. Wang, Y. Li, Y. Li, H. R. Lee, A. Pei, X. He and Y. Cui, *Joule*, **3**, 1080 (2019).
15. S.-H. Choi, G. Nam, S. Chae, D. Kim, N. Kim, W. S. Kim, J. Ma, J. Sung, S. M. Han, M. Ko, H.-W. Lee and J. Cho, *Adv. Energy Mater.*, **9**, 1803121 (2019).
16. W. Go, M.-H. Kim, J. Park, C. H. Lim, S. H. Joo, Y. Kim and H.-W. Lee, *Nano Lett.*, **19**, 1504 (2019).
17. J. Zhang, Z. Yang, J. Qiu and H.-W. Lee, *J. Mater. Chem. A*, **4**, 5802 (2016).
18. W. Tang, Z. Chen, B. Tian, H.-W. Lee, X. Zhao, X. Fan, Y. Fan, K. Leng, C. Peng, M.-H. Kim, M. Li, M. Lin, J. Su, J. Chen, H. Y. Jeong, X. Yin, Q. Zhang, W. Zhou, K. P. Loh and G. W. Zheng, *J. Am. Chem. Soc.*, **139**, 10133 (2017).
19. S. Li, T.-U. Wi, M. Ji, Z. Cui, H.-W. Lee and Z. Lu, *Nano Lett.*, **21**, 1530 (2021).
20. S. Fahad, Z. Wei and A. Kushima, *J. Power Sources*, **506**, 230175 (2021).
21. Y. Lee, J. Lee, J. Lee, K. Kim, A. Cha, S. Kang, T. Wi, S. J. Kang, H.-W. Lee and N.-S. Choi, *ACS Appl. Mater. Interfaces*, **10**, 15270 (2018).
22. M. Pasta, R. Y. Wang, R. Ruffo, R. Qiao, H.-W. Lee, B. Shyam, M. Guo, Y. Wang, L. A. Wray, W. Yang, M. F. Toney and Y. Cui, *J. Mater. Chem. A*, **4**, 4211 (2016).
23. A. Choi, T. Kim, M. H. Kim, S. W. Lee, Y. H. Jung and H.-W. Lee, *Adv. Funct. Mater.*, **32**, 2111901 (2022).
24. S. Lou, Z. Yu, Q. Liu, H. Wang, M. Chen and J. Wang, *Chem*, **6**, 2199 (2020).
25. D. H. S. Tan, A. Banerjee, Z. Chen and Y. S. Meng, *Nat. Nanotechnol.*, **15**, 170, (2020).
26. L. Wang, J. Wang, and P. Zuo, *Small Methods*, **2**, 1700293 (2018).
27. C. Hogrefe, T. Waldmann, M. B. Molinero, L. Wildner, P. Axmann, and M. W. Mehrens, *J. Electrochem. Soc.*, **169**, 050519 (2022).
28. Y. Wu and N. Liu, *Chem*, **4**, 438 (2018).
29. J. H. Um, K. Kim, J. Park, Y.-E. Sung and S. H. Yu, *J. Mater. Chem. A*, **8**, 13874 (2020).
30. W. Tang, X. Yin, S. Kang, Z. Chen, B. Tian, S. L. Teo, X. Wang, X. Chi, K. P. Loh, H.-W. Lee and G. W. Zheng, *Adv. Mater.*, **30**, 1801745 (2018).
31. M. Wan, S. Kang, L. Wang, H.-W. Lee, G. W. Zheng, Y. Cui and Y. Sun, *Nat. Commun.*, **11**, 829 (2020).
32. Y. Jeon, S. Kang, S. H. Joo, M. Cho, S. O. Park, N. Liu, S. K. Kwak, H.-W. Lee and H. K. Song, *Energy Storage Mater.*, **31**, 505 (2020).
33. S. Kim, S. O. Park, M. Y. Lee, J. A. Lee, I. Kristanto, T. K. Lee, D. Hwang, J. Kim, T. U. Wi, H.-W. Lee, S. K. Kwak and N. S. Choi, *Energy Storage Mater.*, **45**, 1 (2022).
34. S. J. Yeom, C. Lee, S. Kang, T.-U. Wi, C. Lee, S. Chae, J. Cho, D. O. Shin, J. Ryu and H.-W. Lee, *Nano Lett.*, **19**, 8793 (2019).
35. Y. Kim, S. J. Yeom, J. Yoo, J. Yun, H.-W. Lee and S. W. Lee, *Nano Lett.*, **22**, 6631 (2022).
36. S. Choi, T. w. Kwon, A. Coskun and J. W. Choi, *Science*, **357**, 279 (2017).
37. T. w. Kwon, J. W. Choi and A. Coskun, *Chem. Soc. Rev.*, **47**, 2145 (2018).
38. M. K. Cho, S. J. You, J. G. Woo, J. C. An, S. Kang, H.-W. Lee, J. H. Kim, C. M. Yang and Y. J. Kim, *Compos. Part B Eng.*, **215**, 108799 (2021).
39. Y. K. Jeong, T. W. Kwon, I. Lee, T. S. Kim, A. Coskun and J. W. Choi, *Nano Lett.*, **14**, 864 (2014).
40. T. w. Kwon, Y. K. Jeong, E. Deniz, S. Y. Alqaradawi, J. W. Choi and A. Coskun, *ACS Nano*, **9**, 11317 (2015).
41. S. Ko, M. J. Baek, T. U. Wi, J. Kim, C. Park, D. Lim, S. J. Yeom, K. Bayramova, H. Y. Lim, S. K. Kwak, S. W. Lee, S. Jin, D. W. Lee and H.-W. Lee, *ACS Mater. Lett.*, **4**, 831 (2022).
42. M. N. Obrovac and V. L. Chevrier, *Chem. Rev.*, **114**, 11444 (2014).
43. S. J. Yeom, T.-U. Wi, S. Ko, C. Park, K. Bayramova, S. Jin, S. W. Lee and H.-W. Lee, *ACS Appl. Mater. Interfaces*, **14**, 5237 (2022).
44. S. Kang, S. J. Yeom and H.-W. Lee, *ChemSusChem*, **13**, 1480 (2020).
45. M. Ko, S. Chae, J. Ma, N. Kim, H.-W. Lee, Y. Cui and J. Cho, *Nat. Energy*, **1**, 16113 (2016).
46. J. A. Lewis, F. J. Q. Cortes, Y. Liu, J. C. Miers, A. Verma, B. S. Vishnugopi, J. Tippens, D. Prakash, T. S. Marchese, S. Y. Han, C. Lee, P. P. Shetty, H.-W. Lee, P. Shevchenko, F. D. Carlo, C. Saldana, P. P. Mukherjee and M. T. McDowell, *Nat. Mater.*, **20**, 503 (2021).
47. J. A. Lewis, C. Lee, Y. Liu, S. Y. Han, D. Prakash, E. J. Klein, H.-W. Lee and M. T. McDowell, *ACS Appl. Mater. Interfaces*, **14**, 4051 (2022).
48. J. E. Lee, K. H. Park, J. C. Kim, T.-U. Wi, A. R. Ha, Y. B. Song, D. Y. Oh, J. Woo, S. H. Kweon, S. J. Yeom, W. Cho, K. S. Kim, H.-W. Lee, S. K. Kwak and Y. S. Jung, *Adv. Mater.*, **34**, 2200083 (2022).
49. C. Lee, S. Y. Han, J. A. Lewis, P. P. Shetty, D. Yeh, Y. Liu, E. Klein, H.-W. Lee and M. T. McDowell, *ACS Energy Lett.*, **6**, 3261 (2021).
50. S. Y. Han, C. Lee, J. A. Lewis, D. Yeh, Y. Liu, H.-W. Lee and M. T. McDowell, *Joule*, **5**, 2450 (2021).
51. Y. B. Song, D. H. Kim, H. Kwak, D. Han, S. Kang, J. H. Lee, S.-M. Bak, K.-W. Nam, H.-W. Lee and Y. S. Jung, *Nano Lett.*, **20**, 4337 (2020).
52. E. Kazyak, R. G-Mendez, W. S. Lepage, A. Sharafi, A. L. Davis, A. J. Sanchez, K.-H. Chen, C. Haslam, J. Sakamoto and N. P. Dasgupta, *Matter*, **2**, 1025 (2020).
53. G. Qiu, L. Lu, Y. Lu and C. Sun, *ACS Appl. Mater. Interfaces*, **12**, 28345 (2020).
54. M. Sun, T. Liu, Y. Yuan, M. Ling, N. Xu, Y. Liu, L. Yan, H. Li, C. Liu, Y. Lu, Y. Shi, Y. He, Y. Guo, X. Tao, C. Liang and J. Lu, *ACS Energy Lett.*, **6**, 451 (2021).
55. G. Zhou, H. Chen and Y. Cui, *Nat. Energy*, **7**, 312 (2022).
56. X. Gao, X. Zheng, J. Wang, Z. Zhang, X. Xiao, J. Wan, Y. Ye, L.-Y. Chou, H. K. Lee, J. Wang, R. A. Vila, Y. Yang, P. Zhang, L.-W. Wang and Y. Cui, *Nano Lett.*, **20**, 5496 (2020).
57. G. Zhou, A. Yang, G. Gao, X. Yu, J. Xu, C. Liu, Y. Ye, A. Pei, Y. Wu, Y. Peng, Y. Li, Z. Liang, K. Liu, L.-W. Wang and Y. Cui, *Sci. Adv.*, **6**, eaay5098 (2020).

Prof. Hyun-Wook Lee is an Associate Professor in the School of Energy and Chemical Engineering at UNIST, South Korea. He received his Ph.D. in Materials Science and Engineering from KAIST, South Korea, in 2012. He was a postdoctoral researcher at Stanford University under supervision of Prof. Yi Cui. His research group at UNIST pursues innovations in lithium/sodium-ion batteries, *operando* imaging observation, cryogenic transmission electron microscopy, Prussian Blue-type redox systems, and electrochemically thermal energy harvesting. His published works in this field have been cited more than 19,000 times, and he was selected as a Highly Cited Researcher in 2019, 2020, 2021, and 2022 by Clarivate Analytics.